

Atomic and energy structure of InAs/AlAs quantum dots

T. S. Shamirzaev,* A. V. Nenashev, A. K. Gutakovskii, A. K. Kalagin, and K. S. Zhuravlev
Institute of Semiconductor Physics, pr. Lavrentieva, 13, Novosibirsk 630090, Russia

M. Larsson and P. O. Holtz

Department of Physics and Measurement Technology, Linköping University, S-581 83 Sweden

(Received 22 May 2008; published 29 August 2008)

The atomic structure and energy spectrum of InAs quantum dots (QDs) in an AlAs matrix have been experimentally studied by transmission electron microscopy (TEM) and steady-state photoluminescence (PL) combined with computational work. The degree of intermixing of InAs and AlAs has been investigated by means of TEM and PL compared with theoretical predictions and found to increase with increasing growth temperature and growth interruption. The band alignment in the QDs is shown to be of type I with the lowest conduction-band states at the direct Γ or at the indirect X_{XY} minima of the QD conduction band, depending on the QD's size and composition.

DOI: [10.1103/PhysRevB.78.085323](https://doi.org/10.1103/PhysRevB.78.085323)

PACS number(s): 73.22.Dj, 78.55.Cr, 78.67.Hc, 61.46.Hk

I. INTRODUCTION

Self-assembled InAs quantum dots (QDs) have been intensively studied in recent years due to their potential significance for fabrication of novel devices.¹ The majority of the studies reported so far have concentrated on the direct-gap In(Ga)As/GaAs material system, while the technologically similar InAs/AlAs system has received much less attention. The system of InAs quantum dots embedded in an AlAs matrix is very close to the InAs/GaAs QDs system what concerns the Stranski-Krastanov growth mode, since AlAs has practically the same lattice constant as GaAs. Nevertheless, the increase in the QD barrier height leads to a stronger electronic confinement in the InAs/AlAs QDs, and to significant changes in their electronic and optical properties as compared to the InAs/GaAs QDs system.²⁻⁴ Recently, microsecond² and even millisecond-scale³ nonexponential photoluminescence (PL) decay have been observed in InAs/AlAs QDs at low temperatures. To explain this long decay several models have been proposed.²⁻⁴ Dawson *et al.*² attributed the long decay times to the recombination involving electrons and holes localized in spatially separated QDs. Later the long PL decay in these QDs was explained in terms of type II indirect transitions of electrons localized in the AlAs matrix with holes localized in the QDs.⁴ These models predict a long PL decay at any temperature, since the recombination probability of spatially separated electrons and holes does not depend on temperature. However, we found that an increase in temperature from 50 to 300 K causes a decrease of the PL decay time in such QDs by 6 orders of magnitude. We demonstrated that this decrease is due to acceleration of the radiative recombination rate and does not relate to thermal activation of fast nonradiative channels.³ An alternative model to “spatially separate carriers” is proposed to explain the thermal dependence of the radiative recombination rate.³ Excitonic levels in small QDs in a high-barrier AlAs matrix splits into an optically active state with a short lifetime (τ_s) and an optically inactive state with a long lifetime (τ_l).^{5,6} The radiative lifetime at low temperatures when kT is less than this splitting (ΔE) is determined by τ_l and at high temperatures ($kT > \Delta E$) by τ_s . However, recently we observed a pro-

longed PL decay at low temperatures even in large InAs/AlAs QDs with a small ΔE .⁷ Thus, a more adequate model explaining the prolonged PL kinetics of the InAs/AlAs QDs at low temperatures and its temperature dependence is required.

In order to construct such a model, we need to establish the electronic structure of the InAs/AlAs QDs, which has been scarcely studied up to now. Hitherto, investigations devoted to studies of the electronic structure of the InAs/AlAs QDs (Refs. 4, 8, and 9) take only the Γ minimum states of conduction band in InAs into consideration. Therefore, two possible configurations of the QDs electronic structure were proposed (i) band alignment of type I with lowest electron states at the Γ minimum of the InAs conduction band and (ii) band alignment of type II, which can be realized if the quantum confinement pushes states at the Γ minimum of the QD conduction band above states at the X minimum conduction band of the matrix.^{4,8,10} In this study of the electronic structure of InAs/AlAs QDs not only the direct Γ minimum but also the indirect L and X minima of the InAs conduction band are taken into account. The effect of confinement on the InAs QDs structures with an indirect band for the electrons has not been studied up to now. Due to the small electron effective mass of InAs, the electron states in the Γ minimum of the QD conduction band are considerably more shifted by confinement than those of the L and X minima. Therefore, the lowest electron states in the QDs can be at the indirect minimum of the conduction band. Actually, we have recently demonstrated that even ultrathin InAs/AlAs quantum wells (QWs) have type I band alignment with lowest electron states at the X minimum of the conduction band.¹¹ Thus, it is reasonable to expect that confinement in InAs/AlAs QDs also results in a transformation from direct to indirect lowest state of the conduction band within the type I band alignment.

In this paper, we present the results of a study of the atomic structure and the energy spectrum of InAs QDs in an AlAs matrix by transmission electron microscopy (TEM), photoluminescence, and computational work. We demonstrate that (i) these QDs consist of an InAlAs alloy with a fraction of InAs, which is dependent on the growth condi-

tions; (ii) the quantum confinement leads to transformation of the lowest electron state from the direct Γ to the indirect X minimum of the InAlAs conduction band, but does not result in a type I to type II transition and (iii) the spectral and temperature dependencies of PL decay time can be explained in terms of a “two levels model.” This model predicts that the lowest energy level of the QDs with long PL lifetime is located at the indirect X minimum and the excited level with short PL lifetime belonging to the direct Γ minimum of the QD’s conduction band.

The paper is organized as follows. In Sec. II, the techniques used for the experimental assessment of the atomic and band structure are described. In Sec. III, the experimental data obtained by transmission electron microscopy and PL to demonstrate intermixing in the InAs/AlAs QDs are presented. Section IV is devoted to revealing electronic and atomic structure of the QDs. We calculate the energy structure of the QDs. A comparison of the calculated energy levels of the optical transitions in the QD with PL data is used for a quantitative estimate of the intermixing degree of InAlAs/AlAs QDs as a function of the growth conditions. In Sec. V, we discuss experimental data on the recombination in InAs/AlAs QDs within the framework of the energy structure of the QDs obtained in this study. Conclusions are given in Sec. VI.

II. EXPERIMENT

The InAs QDs samples studied in this work were grown by molecular-beam epitaxy on semi-insulating (001)-oriented GaAs substrates in a Riber-32P system. The samples consisted of one layer of QDs sandwiched between two 50 nm thick layers of AlAs grown on top of a 200 nm buffer GaAs layer. The first AlAs layer in all the samples was grown at a substrate temperature 600 °C. The QD layers were deposited at a rate $V_G=0.04$ ML s^{-1} (as calibrated in the center of the wafer using reference samples) to a nominal thickness of 2.5 monolayers (MLs). The QDs were formed at temperatures (T_g) varied in the range of 440–540 °C with a growth interruption time (t_{GI}) in the range of 10 to 120 s. The maximum growth interruption time was reduced for samples grown at 530 and 540 °C due to evaporation of In adatoms from the growth surface at high temperatures.¹² The As_4 beam pressure was taken to be about 8.5×10^{-6} Torr except for the sample grown at $T_g/t_{GI}=480$ °C/120 s, where the beam pressure was 4.5×10^{-6} Torr. To prevent InAs evaporation, the growth temperature was not increased during the deposition of the first initial monolayers of the second AlAs layer covering the QDs. The rest of the cover layer was grown at 600 °C. A 20 nm GaAs cap layer was grown on top of the sandwiched QD layer in order to prevent oxidation of AlAs. The size and density of the QDs were studied by means of transmission electron microscopy (employing a JEM-4000EX operated at 200 keV).

The PL excitation was accomplished above the direct band and under the indirect gaps of the AlAs matrix. The PL was excited by a He-Cd laser ($\hbar\omega=3.81$ eV), or a He-Ne laser ($\hbar\omega=1.96$ eV) and a red semiconductor laser ($\hbar\omega=1.87$ eV) with a power density of 30 W cm^{-2} . The detec-

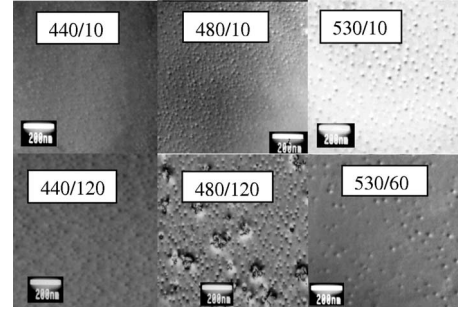


FIG. 1. TEM plane view images of QD samples grown under different temperatures (temperature/interruption time in each figure).

tion of the macro PL was performed by a double diffraction grating spectrometer equipped with a cooled photomultiplier operated in the photon counting mode. In order to select the PL from a single QD, we employed a sample with a small density of QDs ($\sim 10^7$ cm^{-2}) in such a way that only one QD was excited within the laser spot. The excitation in our micro-photoluminescence (μ -PL) system was carried out by a Verdi/MBD266 laser system with a wavelength of 266 nm ($\hbar\omega=4.66$ eV). The laser spot was about 1.5 μm in diameter. The excitation power was varied from 5×10^{-4} to 6 mW. The emission was collected by a microscope, dispersed by a monochromator and detected by a charge coupled device (CCD).

III. INTERMIXING IN InAs/AlAs QUANTUM DOTS

It is well known that strong intermixing of the InAs and the barrier materials will take place for In(Ga)As/Ga(Al)As heterostructures due to the strain-driven InAs segregation.^{13–26} This intermixing is extensively studied for In(Ga)As/GaAs (Refs. 8 and 14–17) and InAs/AlAs (Refs. 11, 17, and 18) QWs. A quantitative phenomenological model of Muraki *et al.*¹⁹ was established for describing the indium composition profile across the QWs. There are also many studies demonstrating intermixing in In(Ga)As/GaAs QDs.^{8,14–17,20–26} While intermixing in InAs/AlAs QDs has been scarcely studied up to now, Ibáñez *et al.* have shown that intermixing takes place in InAs/AlGaAs QDs by the Raman-scattering technique²⁷ and Offerman *et al.* have recently demonstrated a nonuniform InAs/AlAs distribution inside the InAs QDs by cross-sectional scanning tunneling microscopy.⁸ However, there is no systematic study of intermixing phenomena in InAs/AlAs QDs as a function of growth conditions up to date. In this work, we demonstrate that the InAs/AlAs intermixing degree in InAs QDs changes with growth temperature and growth interruption times.

Figure 1 demonstrates TEM plane view images of QD samples grown under different temperatures and interruption times. All samples except one contain only dislocation free QDs. The sample grown at $T_g/t_{GI}=480$ °C/120 s contains both dislocation free QDs and dislocated clusters of InAs, which appear as a result of an increasing In adatoms mobility due to the low As_4 pressure.^{7,28} In order to determine the average diameter (D_{AV}), size dispersion (S_D), and density

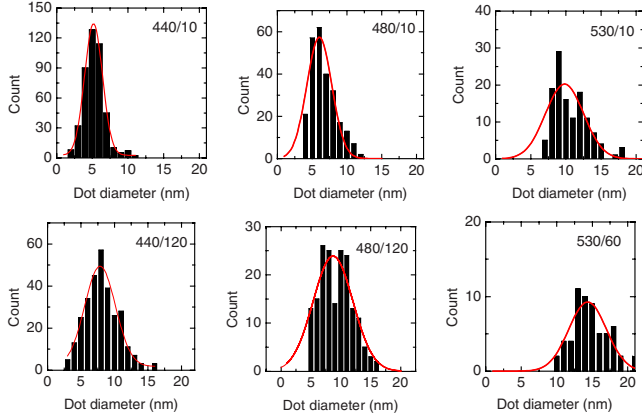


FIG. 2. (Color online) Histograms of the QD size distribution for InAs/AlAs QDs samples grown under different temperatures (temperature/interruption time in each figure). The distribution of the size dispersion is fitted by Gaussian curves. The average dot's diameters and the widths of the dot's diameters distribution (S_D) obtained from these curves are given in Table I.

(D_D) of dislocation free QDs, the diameters and number of QDs are estimated within an area in the range of $0.3\text{--}0.5\ \mu\text{m}^2$. The results are shown in Fig. 2 as histograms, which are used for determination of S_D and D_{AV} of the QDs and are summarized in Table I. One can see that D_{AV} increases and D_D decreases with increasing growth temperature and growth interruption time. These changes in D_{AV} and D_D become especially apparent at higher growth temperatures. It should be noted that the observed values of D_D are larger and the corresponding values of D_{AV} are smaller than for InAs/GaAs QDs formed at similar conditions. These facts have earlier been observed for InAs/AlAs QDs by many groups.^{29–32} However, a specific feature noted here is a higher value of the dot size dispersion for InAs/AlAs QDs.³³ As seen in Table I, the width of Gaussian distribution of the dot size reaches up to almost 40% of the mean QD's diameter, that is considerably larger than typical S_D values (5–20%) for InAs/GaAs QDs.^{34–36}

The formation of the QDs as well as the InAs segregation in both InAs/GaAs and InAs/AlAs systems are determined by kinetic effects on the growth surface.^{16,30,37} Therefore, a

strong variation in D_{AV} , D_D , and S_D between the InAs/GaAs and InAs/AlAs QDs systems denotes a different intermixing rate in these QDs systems. The discussion about mechanisms of intermixing and their difference in InAs/GaAs and InAs/AlAs QDs is out of the framework of our study. In this paper we rather estimate the effect of temperature and growth interruption time on the intermixing degree in InAs/AlAs QDs.

For this purpose, we first make a rough estimation by defining an effective volume occupied by all QDs located within an area of $1\ \text{cm}^2$ as a function of the growth conditions. This effective volume is calculated as the product of D_D and the volume of the QD (with the diameter D_{AV}). To calculate the QD volume, lens shaped QDs with the aspect ratio of 4:1 were selected. In the resulting data (presented in Table I), one can see that in spite of the equal amount of deposited InAs, the effective volume increases by about a factor of 4.5 times with increasing temperature from 440 to 510 °C and a raised growth interruption time, from 10 to 120 s, respectively. We assume that this increase in the effective volume is a result of an increasing intermixing with increasing growth temperature and interruption time. However, a further increase of T_g results in a decreasing effective volume due to evaporation of In adatoms from the surface of the sample.¹²

Low temperature PL spectra of the InAs/AlAs QDs grown at different conditions (Fig. 3) confirm this assumption. Three bands marked WL, QD, and GaAs, presented in the spectra refer to recombination in the wetting layer,¹¹ the QDs, and the GaAs buffer layer, respectively. The energy positions at the maximum ($\hbar\omega_{QD}$) of the QD PL band as a function of growth condition are collected in Table I. For QDs grown with a fixed growth interruption time, an increasing T_g (from 440 to 530 °C) results in redshift of $\hbar\omega_{QD}$. For a fixed T_g , $\hbar\omega_{QD}$ (i) is redshifted for lower growth temperatures ($\leq T_g = 440\ \text{°C}$), (ii) remains almost unshifted for T_g in the range of 480–510 °C and (iii) is blueshifted at higher T_g with increasing growth interruption time. The energy of the PL emission from QDs is primarily determined by the confinement of charge carriers. An invariance or even a blueshift of the PL band with increasing QD size implies that InAs/AlAs intermixing results in an increasing AlAs fraction in the alloy composition of QDs.

TABLE I. Average diameter, size dispersion, density, composition, and spectral parameters of the PL emission for InAs/AlAs QDs.

T_g/t_{GI} °C/s	D_{AV} (nm)	S_D (nm)	S_D % of D_{AV}	$D_D \times$ $10^{10}\ \text{cm}^2$	Volume of QDs on $\text{cm}^2 (\times 10^{11}\ \text{nm}^3)$	Maximum of PL band (eV)	Fraction of InAs (x)
440/10	5.2 ± 0.03	1.7 ± 0.08	33	11.1	20	1.805	0.99
440/120	8.0 ± 0.15	3.0 ± 0.15	37	6.3	40	1.755	0.78
480/10	6.3 ± 0.15	1.8 ± 0.2	30	10	31	1.750	0.93
480/120	8.7 ± 0.05	3.3 ± 0.14	38	6.1	52	1.751	0.73
510/30	10.4 ± 0.04	3.9 ± 0.13	36	3.7	58	1.680	0.75
510/120	12.7 ± 0.01	2.5 ± 0.06	21	3.5	90	1.685	0.68
530/10	9.8 ± 0.06	2.7 ± 0.25	28	2.8	33	1.695	0.73
530/60	14.3 ± 0.03	2.7 ± 0.15	19	0.9	33	1.875	0.42
540/30	18.3					1.856	0.41

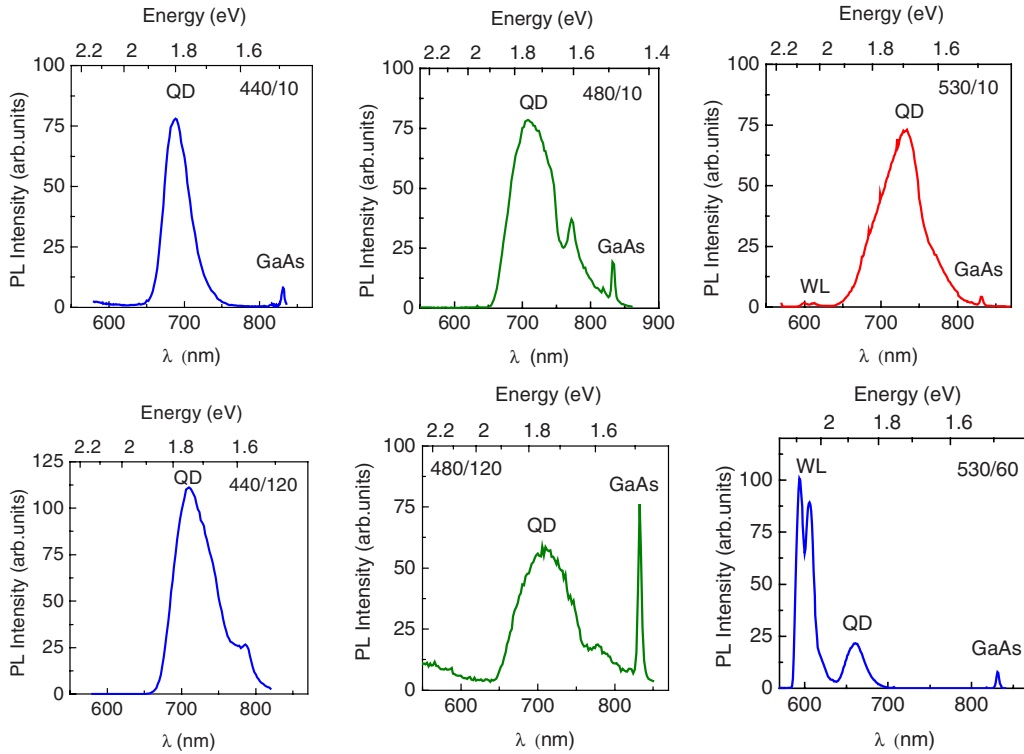


FIG. 3. (Color online) Low temperature (5 K) PL spectra of InAs/AlAs QDs samples grown under different temperatures (temperature/interruption time in each figure).

Below, we estimate the alloy composition of the studied QDs by comparing the energy of the PL transition in the QDs with the calculated energy for the optical transition in the QD using the AIAs fraction of the QD as the variable parameter of the calculations.

IV. ELECTRONIC AND ATOMIC STRUCTURE OF InAs/AlAs QUANTUM DOTS

A. Calculations

The electronic structure of the studied QDs has been calculated by using the nanodevice simulation tool NEXT-NANO3 (Ref. 38). The energy levels of the holes and the electrons in the Γ , X , and L minima of the conduction bands have been calculated by means of a simple band effective-mass approach. The strain, deformation potentials as well as the nonparabolic form of the electron dispersion³⁹ have been taken into account in the calculations. For simplicity, the exciton correction for the energy levels was neglected.

The electronic structure of an InAs/AlAs QD is determined by the size, shape, and chemical composition of the QD, but also by the InAs and AlAs parameters. The diameters of the QDs grown were determined from plane view TEM micrographs, whereas the shape of the QDs was earlier determined from cross-section TEM micrographs.⁴⁰ The QDs were found to be lens like with an aspect ratio varying from 3:1 to 5:1. For our calculations, the aspect ratio of 4:1 was selected.

The chemical composition of the QDs is not known. A nonhomogenous distribution of the InGaAs alloy across the

QDs has been demonstrated in numerous investigations of the composition of In(Ga)As/GaAs QDs.^{8,14,16,21,24,41} Up to date, there are several experimental descriptions of the In-GaAs alloy composition across the QDs. Litvinov *et al.* demonstrated that QDs look like nuclei with a high fraction of InAs in the center surrounded by a shell in which the InAs fraction decreases from the center to the edge of the QDs.¹⁶ On the other hand, Offermans *et al.* demonstrated a monotonic increase in the InAs fraction from the base to the top of the InGaAs/GaAs QD, to reach an InAs fraction of 100% at the dot top.⁸ The difficulty in describing the In diffusion and segregation during the formation of the capped QDs hampers the development of a theoretical model of the alloy composition distribution in the QDs even in the well studied InGaAs/GaAs QDs system. Consequently, the alloy composition distribution is less known in the scarcely studied InAlAs/AlAs QDs. Here we accept that the $\text{In}_x\text{Al}_{1-x}\text{As}$ alloy composition changes inside QD according to a two-dimensional Gaussian function. An InAs concentration maximum is located at the center of the QD, two MLs above its bottom. The InAs fraction (x) decreases along the growth axis through the center of the QD, down to a value 15% below the maximum x , while in the plane two MLs above the QD's bottom perpendicularly to the growth axis, the x value decreases down to a value 10% below the maximum x . An example of such an alloy composition distribution is demonstrated in Fig. 4 for a QD with a maximum InAs fraction of 0.8 and a diameter of 26 nm.

Unfortunately, together with accurately experimentally determined or calculated parameters for InAs and AlAs such as lattice constants, elastic and piezoelectric constants, spin-

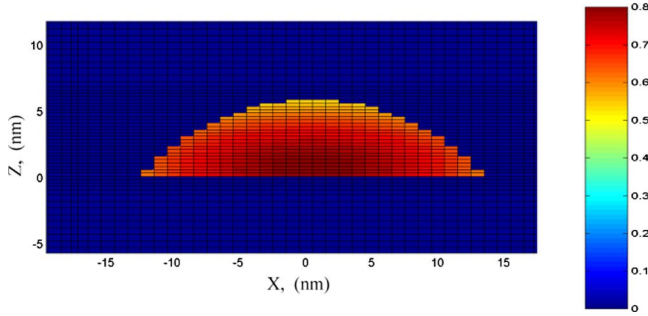


FIG. 4. (Color online) An example of the distribution of the alloy composition across a QD used in the calculations. The scale bar shows the fraction of InAs in the $\text{In}_x\text{Al}_{1-x}\text{As}$ alloy.

orbit splitting, and deformation potentials^{42–47} there are parameters, which are poorly known. These parameters are e.g., the low-temperature energy gaps of the conduction-band minima at X (E_X) and at L (E_L) in InAs, and the valence-band offset (VBO) for an InAs/AlAs heterojunction. For instance, Vurgaftman *et al.* proposed $E_X=1.433$ eV and $E_L=1.133$ eV,⁴⁷ while Ridley *et al.* suggested $E_X=1.39$ eV and $E_L=0.98$ eV (Ref. 48) and Boykin⁴⁹ and Landolt-Bornstein tables⁵⁰ give $E_X=2.27$ eV and $E_L=1.152$ eV, respectively. Also the VBO value for an InAs/AlAs heterojunction is also not well determined. There are many calculations for strained InAs layers on unstrained AlAs substrates, which give various values for the VBO in the range from 0.29 to 0.83 eV.¹¹

In order to choose relevant parameters, we calculated the energy spectrum for a 1.4 ML thick InAs/AlAs QW with a chemical composition profile described by the Muraki model¹⁹ and select available parameters on the E_X , E_L , and VBO (from the literature), which ensure type I band alignment for the QW. Other parameters used in the calculations were taken from Ref. 11. However, the energy of the optical transition in the QW calculated using the selected parameters differs from the experimentally determined energy.¹¹ We found that the energy for the optical transition in the QW is more sensitive to E_X than to the VBO value. The best agreement between the calculated and the experimental results on the energy for the optical transition in the QW was reached for $E_X=1.580$ eV, which is used in the following calculations. The parameters used in calculations are given in Table II.

TABLE II. Selected band-structure parameters for InAs and AlAs used in the calculations.

Parameters	InAs	AlAs
E_Γ (eV)	0.417 ^a	3.099 ^a
E_X (eV)	1.580	2.24 ^a
E_L (eV)	1.33 ^a	2.46 ^a
Valence band edge energy (eV)	0.44 ^b	-0.093 ^b

^aReference 47.

^bReference 45.

B. Calculations of electronic structure of the QD

Calculated energy spectra of the studied QDs with different diameters as a function of composition are presented in Fig. 5. All QDs have a type I band alignment. One can see that related positions of the electronic levels belonging to different minima of the QD conduction band depend on size and composition of the QD. In small QDs (diameter < 7.5 nm), the lowest electronic level is at the X_{XY} minimum of the conduction band independently on the composition. In large QDs with a low AlAs fraction, the electronic level is at the Γ minimum of the conduction band. With increasing AlAs fraction, the electronic states at the Γ minimum shift considerably more than of the states at the X minimum. Accordingly, the states at the Γ and X minima intersect for some composition and the X_{XY} minimum becomes the lowest electronic state in the QDs. The composition corresponding to this intersection depends on the diameter of the QD. Thus, InAs/AlAs QDs can have direct or indirect band structures within the type I band alignment.

C. Atomic structure of the QD

A comparison of the QD PL emission energy with predicted transition energies from the calculations allows us to estimate the composition of the QD. Assuming that photons with the peak energy in the PL spectra (Fig. 3) are emitted from QDs with diameters corresponding to the maximum of the size distribution, we can estimate the InAs fraction in the QDs as a function of the growth conditions (see Table I). We interpolate these data and build a nomogram, as shown in Fig. 6.⁵¹ One can see that QDs grown at low temperature (440 °C) and small interruption time (10 s) consist essentially of pure InAs. An increase in T_g with a maintained growth interruption time causes a decrease in the InAs fraction in the QD down to 0.73 at $T_g=530$ °C. Besides, an increase in the growth interruption time for a fixed T_g leads to a decreasing InAs fraction too. Accordingly, QDs grown at higher temperatures always contain a higher concentration of AlAs.

V. RELATIONSHIP BETWEEN CALCULATED SPECTRA AND EXPERIMENTAL DATA ON THE CARRIERS RECOMBINATION IN InAs/AlAs QDs

In this section we demonstrate that the available experimental data on the carriers recombination for InAs/AlAs QDs are consistent with a type I band alignment based on the calculations in Sec. IV.

A. Micro-PL of InAs/AlAs QD

Recently μ -PL of a single InAs/AlAs QD has been reported by Sarkar *et al.*^{10,52} They observed sharp peaks below 1.8 eV as well as a continuous spectrum above this energy and concluded that this continuous spectrum is due to type II band alignment in small QDs. However, this conclusion is in contradiction to our calculations resulting in a type I band alignment in any InAs/AlAs QDs. In this section, we experimentally demonstrate that InAs/AlAs QDs have type I band

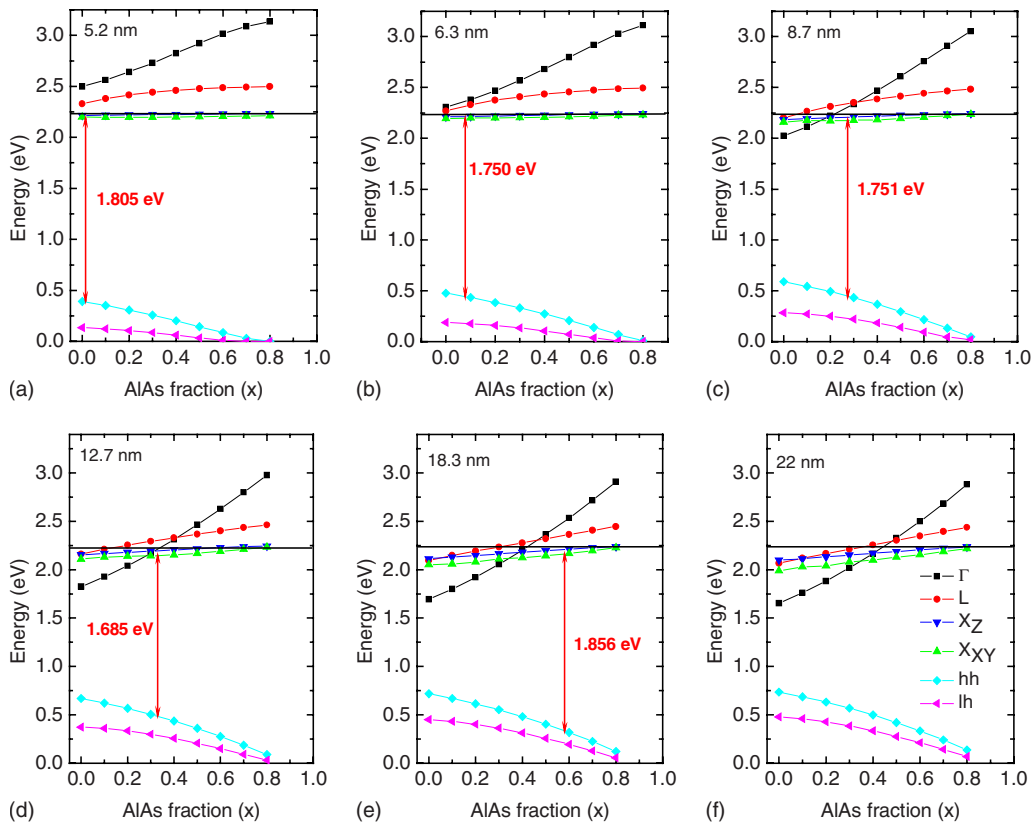


FIG. 5. (Color online) Calculated energy levels of QDs with different diameters as a function of AlAs fraction in the QD. QD diameters: (a) 5.2 nm, (b) 6.3 nm, (c) 8.7 nm, (d) 12.7 nm, (d) 18.3 nm, (e) 22 nm. The reference level is at the top of the AlAs valence band. The labels of the different levels are presented in the figure (e). The horizontal solid line is the bottom edge of the AlAs matrix conduction band. The vertical lines refer to the alloy composition at which the PL emission energy corresponds to the energy of the optical transition in the QD with a corresponding diameter.

alignment even for energies above 1.8 eV. We will also discuss the possible origin of the continuous spectrum.

A method for determination of the band lineup of heterostructures based on the PL technique has been proposed by Ledentsov *et al.*⁵³ They theoretically calculated and experimentally demonstrated that the energy position of the PL band should blueshift proportionally with the cube root of the excitation power density (P) for any structures with type II alignment. The blueshift is characteristic to all type II heterostructures (both QWs and QDs) and reflects the dipole layer formation caused by a spatial separation of nonequilibrium holes confined in the QW or QD and electrons confined in the nearby matrix region.^{53,54} This PL technique was successfully used for many type II systems such as GaSb/GaAs QWs and QDs,^{53,54} GaAs/AlAs QWs,¹¹ InAs/GaAs QDs at high hydrostatic pressure⁵⁵ and ZnMnTe/ZnSe QDs.⁵⁶

μ -PL spectra of the InAs/AlAs QDs specimen grown at $T_g/t_{GI}=540^\circ\text{C}/30\text{ s}$ as a function of excitation power density are depicted in Fig. 7. A PL band (labeled as QD₀) with a maximum at 1.815 eV and with a full width at half maximum (FWHM) of 14 meV, related to the recombination of electrons and holes in the QD, is observed in the μ -PL spectrum at an excitation power of $P=1\text{ kW}/\text{cm}^2$. We believe that the QD₀ band is due to the emission of a single QD since (i) TEM data exhibit a dots density of about 10^7 cm^{-2} (inset in Fig. 7) and (ii) a small shift ($\sim 1\ \mu\text{m}$) of the excited laser

spot results in a jump in the energy position of the QD₀ band by 70 meV due to the fact that another QD is monitored. A large PL linewidth from a single QD was previously observed in different QD systems such as InP/InGaP,⁵⁷ CdSe/ZnS,⁵⁸ and Si.⁵⁹ It has been demonstrated that the PL linewidth associated with the indirect band gap QD is larger

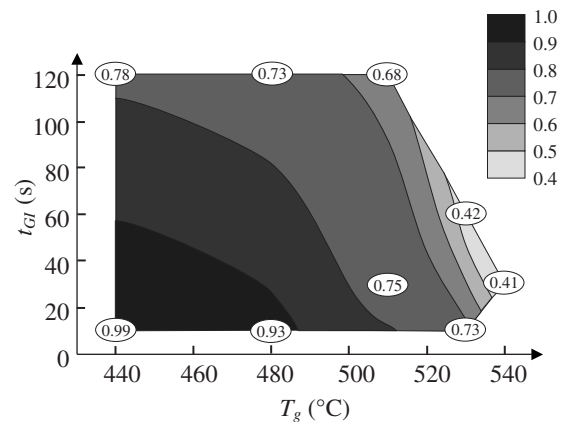


FIG. 6. A nomogram of InAs fraction in QDs as a function of growth temperature and time interruption. The scale bar shows fraction of InAs (x) in the $\text{In}_x\text{Al}_{1-x}\text{As}$ alloy. The numbers in the plane of the picture mark the InAs fraction in the studied QDs.

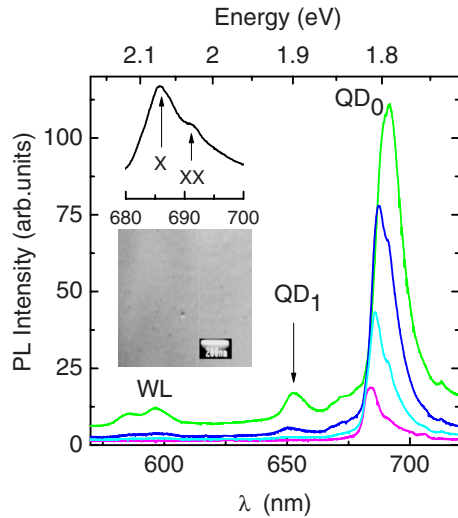


FIG. 7. (Color online) μ -PL spectra of a single InAs/AlAs QD as a function of power density. P top-down kW/cm^2 : 80, 19, 9, 1. Insets demonstrate: (upper) QD_0 and XX lines at $P=9 \text{ kW}/\text{cm}^2$, (lower) TEM plane view images of the sample. A temperature of 60 K was established.

than for the corresponding PL associated with a QD with a direct band gap.⁵⁹

Upon an increasing excitation power, additional bands (labeled WL, XX, and QD in Fig. 7) will appear in the μ -PL spectra. The intensities of these bands will increase more with increasing excitation power than the QD_0 band. The WL energy position is consistent with the recombination of the wetting layer.¹¹ The XX band exhibits a square dependence on the excitation power and becomes dominating the PL spectra for $P > 40 \text{ kW}/\text{cm}^2$. This fact together with the 9 meV redshift of the XX band with respect to the QD_0 strongly indicates that the XX band is due to the recombination of the biexciton.¹⁰ The QD_1 emission is proposed to be due to the recombination of excitons originating from the excited levels of the studied QD.

The dependencies of the PL band shift on the excitation power for the InAs/AlAs QD and type II GaAs/AlAs QW taken from our recent study¹¹ are shown in Fig. 8. The en-

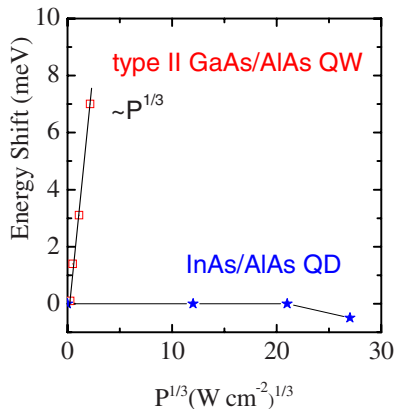


FIG. 8. (Color online) The shift of the PL lines of the InAs/AlAs QD and type II GaAs/AlAs QW as a function of excitation power density P .

ergy position of the QD_0 band is independent on the excitation power for $P < 9 \text{ kW}/\text{cm}^2$. A small redshift of the PL band for further increased excitation power is due to an increase in the relative intensity of multiparticles excitons PL bands.⁶⁰ On the other hand, the PL of the type II GaAs/AlAs QW exhibits a blueshift proportional to the cubic root of the excitation power, in good agreement with predictions.^{53,54}

Accordingly, the observed dependence of the PL band shift on the excitation density unambiguously implies a type I alignment for the band structure of the studied InAs/AlAs QD, which is in agreement with our calculations, but in contrast with the conclusion by Sarkar *et al.*¹⁰ We believe that the reason for this discrepancy is due to the fact that the indirect minima of the QD conduction band were not taken into account by Sarkar *et al.*¹⁰ The continuous spectrum observed in Ref. 10 is not due to the type II alignment of the QD, but rather associates with overlapping broad bands of a few QDs with indirect band gap.

It is interesting that the PL spectrum of the InAs/AlAs QD with an indirect band gap exhibits only one (zero-phonon) band, while the corresponding PL spectrum of a InAs/AlAs QW with a similar electronic structure contains several phonon replicas. A single emission band without phonon replicas was recently observed in PL spectra for an indirect band-gap single Si QD.⁵⁹ That is typical for indirect band-gap QDs due to a strong three-dimensional (3D) confinement, which breaks down the k -conservation rule and results in an increased intensity of the zero-phonon PL band^{59,61} and could explain the predominance of the zero-phonon band in the PL spectra of small InAs QDs.

B. Steady state PL as a function of excitation energy

The PL of InAs/AlAs QDs as a function of excitation energy (E_{EX}) has been investigated. For excitation with energies above the band gap of the AlAs matrix, the PL band involving the QDs will appear in the spectra of all studied samples. However, decreasing the excitation energy to $E_{\text{EX}} < 1.96 \text{ eV}$ divides the samples into two groups: (i) The samples showing high-energy PL bands (1.805, 1.856, and 1.875 eV) for above band-gap excitation, but do not show any PL for below band-gap excitation. (ii) The other samples demonstrate PL spectra similar to those depicted in Fig. 9 (for the sample grown at $T_g/t_{\text{GI}}=480 \text{ }^\circ\text{C}/10 \text{ s}$). For decreasing excitation energy, E_{EX} from 3.81 to 1.96 eV and below for constant excitation power, the PL intensity will decrease several orders of magnitude. The shape of the PL spectra also changes with the excitation energy. A broad unstructured PL band observed upon excitation above the AlAs band gap changes to a series of relatively sharp lines superimposed on a background band upon excitation below the band gap. The lines demonstrate a Stokes shift, which decreases with decreasing excitation energy E_{EX} . These facts were earlier observed for InAs/AlAs QDs by Dawson *et al.*⁴ They demonstrated that these sharp lines appearing in the spectra are due to the resonant absorption in excited levels of the QDs.

In order to explain these experimental results, we construct an energy diagram of the InAs/AlAs QD as a function of the dot's diameter. An energy diagram for QDs with

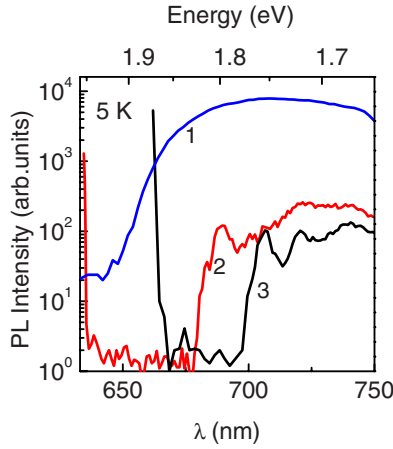


FIG. 9. (Color online) Low temperature (5 K) PL spectra of InAs/AlAs QDs measured at different energy of excitation light: 1–3.81 eV, 2–1.96 eV, 3–1.87 eV.

different sizes with an InAs fraction $x=0.9$ i.e., close to the composition of the sample grown at $T_g/t_{GI}=480$ °C/10 s is shown in Fig. 10. We will next consider the generation and recombination of charge carriers in the framework of this diagram. When the excitation energy E_{EX} exceeds the band gap of AIAs, electrons and holes are generated in the matrix. Subsequently, the carriers will become captured and recombine in QDs of all sizes, which result in a broad unstructured band in the PL spectra. On the other hand, for E_{EX} below the band gap of AIAs, carriers can only be excited from QD's levels. Light absorption in thin QD's layer is much smaller than for a thick AIAs matrix, which subsequently results in a strong decrease of the PL intensity for the low energy excitation. According to selection rules, a significant contribution of the absorption of photons with an energy below the barrier band gap, gives rise to transitions between the heavy-hole level (E_{hh}^{QD}) and the electronic level at the Γ minimum of the

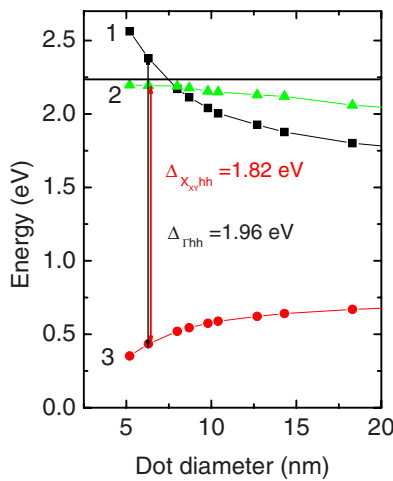


FIG. 10. (Color online) Band energy structure for QDs with an InAs concentration of $x=0.9$ as a function of the QD diameter. The energy is given relatively the top of the AIAs valence band. The horizontal solid line represents the edge of the AIAs conduction band. The numerals refer to: 1- Γ , 2- X_{XY} , electronic levels and 3 - heavy hole levels.

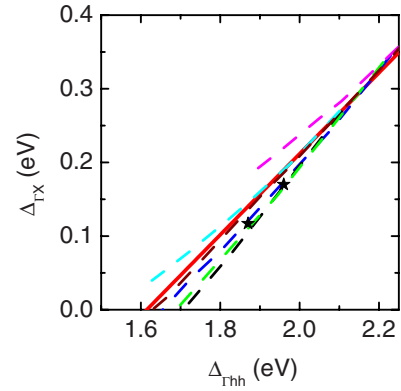


FIG. 11. (Color online) $\Delta_{\Gamma X}$ versus $\Delta_{\Gamma hh}$ in an array of $In_xAl_{1-x}As/AlAs$ QDs with different sizes. The different InAs fractions x are illustrated by the dashed lines: black—1, green—0.9, blue—0.8, brown—0.7, cyan—0.6, and magenta—0.5. The red solid line corresponds to experimental data from Ref. 4. The stars refer to our experimental data for $In_{0.93}Al_{0.07}As/AlAs$ QDs.

QD's conduction band (E_{Γ}^{QD}). The energy difference between these levels is $\Delta_{\Gamma hh} = E_{\Gamma}^{QD} - E_{hh}^{QD}$. Meanwhile for small size QDs, the recombination occurs between the lowest electronic level at the X_{XY} minimum of the QD's conduction band (E_{XY}^{QD}) and the heavy-hole level. The energy difference between these levels is $\Delta_{Xhh} = E_{XY}^{QD} - E_{hh}^{QD}$. Therefore, QDs with $\Delta_{\Gamma hh} > E_{EX}$ do not emit even if E_{EX} exceeds Δ_{Xhh} . For QDs with $\Delta_{\Gamma hh} = E_{EX}$, a resonant excitation can occur, that results in the appearance of a sharp PL line. The Stokes shift of the line equals the difference between E_{Γ}^{QD} and E_{XY}^{QD} ($\Delta_{\Gamma X}$). For large size QDs, the resonant excitation in the excited states at the Γ minimum of the QD's conduction band gives rise to several sharp lines in the PL spectrum of the QD's array.⁴

Figure 11 shows $\Delta_{\Gamma X}$ versus $\Delta_{\Gamma hh}$ for QDs with different diameters and composition, based on our calculations. In a QDs array, $\Delta_{\Gamma X}$ decreases with an increasing QD's diameter due to decreasing $\Delta_{\Gamma hh}$ down to zero at the intersection points of the Γ and X_{XY} minima of the QD's conduction band. For comparison, the curve obtained by Dawson *et al.*⁴ with fitting of their experimental data as well as our experimental data are presented in the same figure. As can be seen, a nice agreement between the experimental results and the predictions based on our calculations is achieved. A best fit to our experimental data is achieved by the curve related to the QDs with an InAs fraction of $x=0.9$, while the experimental data of Dawson *et al.*⁴ represents an InAs fraction of $x=0.70$, which reflects the difference in growth conditions for the arrays of QDs.

C. Spectral and temperature dependencies of PL kinetics

The indirect-direct transition in the band energy structure with increasing QDs size, appearing also in the PL kinetics of an InAs/AlAs QDs array as an abrupt acceleration of PL decay at low energy region of QD PL band.^{4,62} It is interesting that for a fixed temperature, the PL decay demonstrated a monotonic acceleration with an associated redshift of the spectrum (i.e., an increasing QDs size) before slump into the direct-band-gap QDs.⁴ A similar monotonic acceleration of

the PL decay observed at the high-energy region of the QD PL band for increasing temperatures.³ Calculated energy spectra of InAs/AlAs QDs allow us to qualitatively explain the observed monotonic acceleration of the PL kinetics. In accordance with the data on QD's sizes and composition presented in Table I, most QDs in the studied structures have the lowest electronic level at the X_{XY} minimum and the excited electronic level at the Γ minimum of the conduction band. For small QDs, the radiative lifetime at low temperatures ($kT \ll \Delta_{\Gamma X}$) is determined by a long lifetime of an electron located in the indirect QD conduction band. For an increasing kT relatively $\Delta_{\Gamma X}$ with increasing QDs diameter or increasing temperature, a redistribution of electrons between the lower and excited states in the QD will occur. Due to an increasing fraction of carriers that will recombine from an electronic level at the Γ minimum of the conduction band, the PL decay will be shortened to the nanosecond region.

VI. CONCLUSION

The atomic and electronic structure of InAs QDs in an AlAs matrix has been investigated. We have shown that only

QDs grown at low temperatures and with short growth interruption times consist of essentially pure InAs, while an increase of any or both of these parameters results in a strong InAs-AlAs intermixing. It has been concluded that the QDs have a type I band alignment, while the lowest electron state of the QDs can be at either the direct Γ or at the indirect X minima of the QD conduction band, depending on the size and composition of the QD. The spectral and temperature dependencies of the PL kinetics of the InAs/AlAs QDs are explained in terms of an electron redistribution between long-lived indirect and short-lived direct states of the QDs conduction band.

ACKNOWLEDGMENTS

This work was supported by the RFBR (Grants No. 07-02-00134 and No. 06-02-16988) and by Dynasty Foundation. K. S. Zhuravlev thanks the Royal Swedish Academy of Sciences for the financial support.

*timur@thermo.isp.nsc.ru

- ¹D. Bimberg, M. Grundmann, and N. Ledentsov, *Quantum Dot Heterostructures* (Wiley, New York, 1999).
- ²P. Dawson, Z. Ma, K. Pierz, and E. O. Göbel, *Appl. Phys. Lett.* **81**, 2349 (2002).
- ³T. S. Shamirzaev, A. M. Gilinsky, A. I. Toropov, A. K. Bakarov, D. A. Tenne, K. S. Zhuravlev, C. von Borczyskowski, and D. R. T. Zahn, *JETP Lett.* **77**, 389 (2003).
- ⁴P. Dawson, E. O. Göbel, and K. Pierz, *J. Appl. Phys.* **98**, 013541 (2005).
- ⁵S. V. Gupalov and E. L. Ivchenko, *Phys. Solid State* **42**, 2030 (2000).
- ⁶H. Fu, L.-W. Wang, and A. Zunger, *Phys. Rev. B* **59**, 5568 (1999).
- ⁷T. S. Shamirzaev, A. M. Gilinsky, A. K. Kalagin, A. I. Toropov, A. K. Gutakovskii, and K. S. Zhuravlev, *Semicond. Sci. Technol.* **21**, 527 (2006).
- ⁸P. Offermans, P. M. Koenraad, J. H. Wolter, K. Pierz, M. Roy, and P. A. Maksym, *Phys. Rev. B* **72**, 165332 (2005).
- ⁹A. J. Williamson, A. Franceschetti, H. Fu, L. W. Wang, and A. Zunger, *J. Electron. Mater.* **28**, 414 (1999).
- ¹⁰D. Sarkar, H. P. van der Meulen, J. M. Calleja, J. M. Becker, R. J. Haug, and K. Pierz, *Phys. Rev. B* **71**, 081302(R) (2005).
- ¹¹T. S. Shamirzaev, A. M. Gilinsky, A. K. Kalagin, A. V. Nenashev, and K. S. Zhuravlev, *Phys. Rev. B* **76**, 155309 (2007).
- ¹²C. Heyn and W. Hansen, *J. Cryst. Growth* **251**, 218 (2003).
- ¹³S. Martini, A. A. Quivy, T. E. Lamas, and E. C. F. da Silva, *Phys. Rev. B* **72**, 153304 (2005).
- ¹⁴A. Rosenauer, W. Oberst, D. Litvinov, D. Gerthsen, A. Forster, and R. Schmidt, *Phys. Rev. B* **61**, 8276 (2000).
- ¹⁵A. Rosenauer, D. Gerthsen, D. Van Dyck, M. Arzberger, G. Böhm, and G. Abstreiter, *Phys. Rev. B* **64**, 245334 (2001).
- ¹⁶D. Litvinov, D. Gerthsen, A. Rosenauer, M. Schowalter, T. Passow, P. Feinaugle, and M. Hetterich, *Phys. Rev. B* **74**, 165306

(2006).

- ¹⁷P. Offermans, P. M. Koenraad, R. Notzel, J. H. Wolter, and K. Pierz, *Appl. Phys. Lett.* **87**, 111903 (2005).
- ¹⁸M. Schowalter, A. Rosenauer, D. Gerthsen, M. Arzberger, M. Bichler, and G. Abstreiter, *Appl. Phys. Lett.* **79**, 4426 (2001).
- ¹⁹K. Muraki, S. Fukatsu, Y. Shiraki, and R. Ito, *Appl. Phys. Lett.* **61**, 557 (1992).
- ²⁰X. Z. Liao, J. Zou, D. J. H. Cockayne, R. Leon, and C. Lobo, *Phys. Rev. Lett.* **82**, 5148 (1999).
- ²¹N. Liu, J. Tersoff, O. Baklenov, A. L. Holmes, Jr., and C. K. Shih, *Phys. Rev. Lett.* **84**, 334 (2000).
- ²²A. Lemaître, G. Patriarche, and F. Glas, *Appl. Phys. Lett.* **85**, 3717 (2004).
- ²³P. D. Quinn, N. R. Wilson, S. A. Hatfield, C. F. McConville, G. R. Bell, T. C. Q. Noakes, P. Bailey, S. Al-Harhi, and F. Gard, *Appl. Phys. Lett.* **87**, 153110 (2005).
- ²⁴T. Walther, A. G. Cullis, D. J. Norris, and M. Hopkinson, *Phys. Rev. Lett.* **86**, 2381 (2001).
- ²⁵P. Wang, A. L. Bleloch, M. Falke, P. J. Goodhew, J. Ng, and M. Missous, *Appl. Phys. Lett.* **89**, 072111 (2006).
- ²⁶T. Passow, S. Li, P. Feinaugle, T. Vallaitis, J. Leuthold, D. Litvinov, D. Gerthsen, and M. Hetterich, *J. Appl. Phys.* **102**, 073511 (2007).
- ²⁷J. Ibáñez, R. Cuscó, L. Artús, M. Henini, A. Patané, and L. Eaves, *Appl. Phys. Lett.* **88**, 141905 (2006).
- ²⁸N. A. Cherkashin *et al.*, *Semiconductors* **37**, 861 (2003).
- ²⁹F. Ferdos, S. Wang, Y. Wei, M. Sadeghi, Q. Zhao, and A. Larson, *J. Cryst. Growth* **251**, 145 (2003).
- ³⁰P. Ballet, J. B. Smathers, H. Yang, C. L. Workman, and G. J. Salamo, *J. Appl. Phys.* **90**, 481 (2001).
- ³¹S. Park, J. Tatebayashi, and Y. Arakawa, *Appl. Phys. Lett.* **84**, 1877 (2004).
- ³²K. Pierz, Z. Ma, I. Hapke-Wurst, U. Keyser, U. Zeitler, and R. Haug, *Physica E (Amsterdam)* **13**, 761 (2002).

- ³³The large size dispersion appears also as a large linewidth FWHM achieves 180 meV of the QDs PL band. In our case, the FWHM of PL bands and, therefore, dispersion are in several times larger than for InAs/GaAs QDs [see, for example, H. Heidemeyer, S. Kiravittaya, C. Muller, N. Y. Jin-Phillipp, and O. G. Schmidt, *Appl. Phys. Lett.* **80**, 1544 (2002); T. Yang, J. Tatebayashi, S. Tsukamoto, M. Nishioka, and Y. Arakawa, *ibid.* **84**, 2817 (2004); E. C. Le Ru, P. Howe, T. S. Jones, and R. Murray, *Phys. Rev. B* **67**, 165303 (2003); H. Z. Song, T. Usuki, Y. Nakata, N. Yokoyama, H. Sasakura, and S. Muto, *ibid.* **73**, 115327 (2006)].
- ³⁴P. B. Joyce, T. J. Krzyzewski, G. R. Bell, T. S. Jones, S. Malik, D. Childs, and R. Murray, *Phys. Rev. B* **62**, 10891 (2000).
- ³⁵R. Songmuang, S. Kiravittaya, M. Sawadsaringkarn, S. Panyakeow, and O. Schmidt, *J. Cryst. Growth* **251**, 166 (2003).
- ³⁶V. G. Dubrovskii, G. E. Cirlin, and V. M. Ustinov, *Phys. Rev. B* **68**, 075409 (2003).
- ³⁷K. Pierz, Z. Ma, U. F. Keyser, and R. J. Haug, *J. Cryst. Growth* **249**, 477 (2003).
- ³⁸The NEXTNANO3 software package can be downloaded from www.wsi.tum.de/nextnano3 and www.nextnano.de
- ³⁹O. E. Kane, *J. Phys. Chem. Solids* **1**, 249 (1957).
- ⁴⁰A. G. Milekhin, A. I. Toropov, A. K. Bakarov, D. A. Tenne, G. Zanelatto, J. C. Galzerani, S. Schulze, and D. R. T. Zahn, *Phys. Rev. B* **70**, 085314 (2004).
- ⁴¹G. Biasiol, S. Heun, G. B. Golinelli, A. Locatelli, T. O. Menten, F. Z. Guo, C. Hofer, C. Teichert, and L. Sorba, *Appl. Phys. Lett.* **87**, 223106 (2005).
- ⁴²C. G. Van de Walle, *Phys. Rev. B* **39**, 1871 (1989).
- ⁴³S. de Gironcoli, S. Baroni, and R. Resta, *Phys. Rev. Lett.* **62**, 2853 (1989).
- ⁴⁴M. C. Muñoz and G. Armelles, *Phys. Rev. B* **48**, 2839 (1993).
- ⁴⁵S. H. Wei and A. Zunger, *Appl. Phys. Lett.* **72**, 2011 (1998).
- ⁴⁶S. H. Wei and A. Zunger, *Phys. Rev. B* **60**, 5404 (1999).
- ⁴⁷I. Vurgaftman, J. R. Meyer, and L. R. Ram-Mohan, *J. Appl. Phys.* **89**, 5815 (2001).
- ⁴⁸B. K. Ridley, *J. Appl. Phys.* **48**, 754 (1977).
- ⁴⁹T. B. Boykin, *Phys. Rev. B* **56**, 9613 (1997).
- ⁵⁰*Numerical Data and Functional Relationships in Science and Technology*, Landolt-Börnstein, New Series, Group III, Vol. 17, edited by O. Madelung, H. Weiss, and M. Schulz (Springer, Heidelberg, 1982).
- ⁵¹Composition of QDs form at fixed temperature with a t_{GI} determined via linear interpolation between the minimal and the maximal values of t_{GI} . The interruption times correspond to QDs with compositions, x equal to $0.1n$, where n can be taken from 4 to 10 selected as reference points for each T_g . Then the points with equal composition x are connected by B-spline lines.
- ⁵²In order to select PL of a single QD in array the samples studied in Ref. 10 were covered by an aluminium mask containing small square apertures fabricated by electron-beam lithography.
- ⁵³N. N. Ledentsov, J. Böhrer, M. Beer, F. Heinrichsdorff, M. Grundmann, D. Bimberg, S. V. Ivanov, B. Ya. Meltser, S. V. Shaposhnikov, I. N. Yassievich, N. N. Faleev, P. S. Kop'ev, and Zh. I. Alferov, *Phys. Rev. B* **52**, 14058 (1995).
- ⁵⁴F. Hatami *et al.*, *Appl. Phys. Lett.* **67**, 656 (1995).
- ⁵⁵I. E. Itskevich, S. G. Lyapin, I. A. Troyan, P. C. Klipstein, L. Eaves, P. C. Main, and M. Henini, *Phys. Rev. B* **58**, R4250 (1998).
- ⁵⁶M. C. Kuo *et al.*, *Appl. Phys. Lett.* **89**, 263111 (2006).
- ⁵⁷P. G. Blome, M. Wenderoth, M. Hübner, R. G. Ulbrich, J. Porsche, and F. Scholz, *Phys. Rev. B* **61**, 8382 (2000).
- ⁵⁸S. A. Empedocles, D. J. Norris, and M. G. Bawendi, *Phys. Rev. Lett.* **77**, 3873 (1996).
- ⁵⁹I. Sychugov, R. Juhasz, J. Valenta, and J. Linnros, *Phys. Rev. Lett.* **94**, 087405 (2005).
- ⁶⁰It was recently demonstrated that type I In(Ga)As/GaAs QDs exhibit a redshift of the PL band with increasing excitation density. This effect was observed for a QDs array [S. Raymond, X. Guo, J. L. Merz, and S. Fafard, *Phys. Rev. B* **59**, 7624 (1999)]. Besides, for a single QD increasing excitation density leads to appearance of additional PL bands redshifted relatively to the X_0 excitonic transition [E. Dekel, D. V. Regelman, D. Gershoni, E. Ehrenfreund, W. V. Schoenfeld, and P. M. Petroff, *ibid.* **62**, 11038 (2000)]. The relative intensity of these bands strongly increases with increasing excitation power density [D. V. Regelman, U. Mizrahi, D. Gershoni, E. Ehrenfreund, W. V. Schoenfeld, and P. M. Petroff, *Phys. Rev. Lett.* **87**, 257401 (2001)]. These bands were explained in terms of the recombination of multiparticle neutral and charged excitons [see for example E. Dekel, D. Gershoni, E. Ehrenfreund, D. Spektor, J. M. Garcia, and P. M. Petroff, *ibid.* **80**, 4991 (1998); M. Lomascolo, A. Vergine, T. K. Johal, R. Rinaldi, A. Passaseo, R. Cingolani, S. Patanè, M. Labardi, M. Allegrini, F. Troiani, and E. Molinari, *Phys. Rev. B* **66**, 041302(R) (2002)]. In our case, a redshift is due to the appearance of additional low energy PL bands with high FWHM.
- ⁶¹D. Kovalev, H. Heckler, M. Ben-Chorin, G. Polisski, M. Schwartzkopff, and F. Koch, *Phys. Rev. Lett.* **81**, 2803 (1998).
- ⁶²T. S. Shamirzaev, A. Nenashev, and K. S. Zhuravlev, *Appl. Phys. Lett.* **92**, 213101 (2008).